Vol. 16 (2026): Proceedings of the 2026 International Conference on AI and Technological Innovation Applications (AITIA 2026)
E-ISSN: 3105-0522 P-ISSN: 3105-0514
DOI: https://doi.org/10.70267/aitia.202688101

Three-Dimensional UAV Trajectory Planning Based on a Multi-Strategy Chaotic Enhanced Grey Wolf Optimizer

Junyu Ouyang*

College of Transportation Engineering, Dalian Maritime University, Dalian 116026, China

**Corresponding author: Junyu Ouyang.*

Abstract

A Multi-Strategy Chaotic Enhanced Grey Wolf Optimizer (MSCEGWO) is proposed to address the problem of easily falling into local optima, low computational accuracy, and slow convergence speed in the 3D trajectory planning process of unmanned aerial vehicles using the classical Grey Wolf Optimizer (GWO). This algorithm first employs a tent-logistic hybrid map to generate a diverse initial population, expanding the search space; Then, a nonlinear parameter is adopted to update the algorithm parameters, enhancing the global exploration ability of the algorithm; Finally, the golden sine strategy is introduced to prevent the algorithm from trapping into local optima and facilitate the search for more accurate solutions. The improved algorithm is compared with five mainstream swarm intelligence algorithms on ten benchmark functions to verify its effectiveness. Using a real Digital Elevation Model (DEM) as the test environment, the simulation results of three-dimensional trajectory planning using the improved algorithm and other swarm intelligence algorithms are presented, which demonstrate the superiority of the algorithm in solving practical engineering problems.

Keywords

unmanned aerial vehicle (UAV), three-dimensional trajectory planning, multi-strategy chaos-enhanced Grey Wolf Optimizer, chaotic map, golden sine strategy, nonlinear parameter adjustment

1. Introduction

With the rapid development of unmanned aerial vehicle (UAV) technology, the applications of UAVs in both civil and military sectors continue to expand [1]. In terms of civil use, drones have been widely used in rescue and disaster relief, logistics, power line inspection, urban surveying, etc.; In terms of military use, unmanned aerial vehicles have also shown important value in patrol missions, reconnaissance and surveillance and other tasks. However, UAVs often need to complete autonomous navigation under complex three-dimensional space constraints, random distribution of obstacles, no-fly zones and other restrictions to generate a safe, efficient, feasible three-dimensional track that meets various constraints, which is the key technology of autonomous flight of drones.

The path planning method is divided into traditional solution algorithms and swarm intelligence algorithms. Traditional path planning algorithms, such as A*, Dijkstra, RRT, etc., have better planning effect in a twodimensional environment. However, in a complex three-dimensional environment, it often faces problems such as low computing efficiency, slow convergence speed, and poor planning effect.[2] It is difficult to meet the needs of multiple goals such as path length, altitude constraints, flight safety and flight efficiency at the same time. Against this background, researchers began to explore intelligent optimization algorithms inspired by natural phenomena or biological behaviors [3], such as Grey Wolf Optimizer [4] (GWO), Ant Colony Optimization [5] (ACO) and Particle Swarm Optimization Algorithm [6] (PSO). This swarm intelligence algorithm realizes complex optimization problems through mutual collaboration and information exchange between a large number of simple individuals. It has the advantages of simple structure, few parameters and fast convergence speed, so it is widely used in three-dimensional UAV path planning. Domestic scholars have also proposed improved and more efficient group intelligence optimization algorithms: Qin Dongyan [7] et al. choose to use improved nonlinear convergence factors, which improves the robustness of the gray wolf optimization algorithm; Chen Mingqiang [8] et al. integrated the idea of greedy algorithm into the target bias strategy, which reduced the invalid search for sampling points in the RRT* algorithm; Shen Chaoping [9] et al. introduced elite ant colony update strategies into the ant colony algorithm to enhance the exploration ability of subsequent ant colonies; Liu Wenqiang [10] et al. used the population switching strategy, and the individual behavior of the same numbered beetles was no longer fixed, which improved the ability of global exploration and local mining of the algorithm.

The gray wolf optimization algorithm is an intelligent optimization algorithm proposed by Mirjalili [4] in 2014. It is inspired by the social hierarchy structure and collaborative hunting behavior of gray wolves in nature [11]. Because of its simple structure, few parameters and strong global search ability, it has gradually become a research hotspot and is widely used in various fields. Wang Shuqin [12] et al. combined the advantages of global convergence of the gray wolf optimization algorithm to apply it to the optimization of parameters in long-term and short-term memory networks; Bao Xinyu [13] et al. applied the gray wolf algorithm to optimize the parameters of the PID controller to find the optimal solution in the wolf population in the search space to optimize the control of the system. It can be seen that GWO has the advantages of fast convergence speed and high optimization accuracy. However, GWO also has problems such as prone to falling into local optima, uneven distribution of search areas, and low accuracy of optimal solutions. Based on these problems, scholars have carried out a lot of research on the basis of traditional GWO. Wang Qi [14] et al. designed a multi-dimensional collaboratively optimized IGWO algorithm. In the search for the optimal solution, the accuracy of the improvement solution in the algorithm was effectively improved through the differential evolution variation strategy; Wang Haiqun [15] et al. proposed a hybrid gray wolf optimization algorithm CLGWO, which improves the linear convergence factor in the search process and introduces nonlinearity to expand the global search range of the population.

This paper proposes a Multi-Strategy Chaotic Enhanced Grey Wolf Optimizer (MSCEGWO), which uses tent-logistic hybrid mapping, nonlinear update parameters and golden sine strategy to improve its performance. The main work includes: using Tent–Logistic chaotic mapping to generate more random initial populations in the population initialization stage to expand the search scope of the algorithm, using nonlinear functions to update algorithm parameters in the exploitation stage to expand the global exploration ability of the algorithm; Finally, use the golden sine strategy to prevent the algorithm from falling into the local optima. And the improved MSCEGWO is based on the CEC2005 test set of 10 benchmark functions to evaluate the performance of MSCEGWO and compare and analyze it with the GOA, DBO, GWO, PSO and SSA algorithms to prove the effectiveness and superiority of the improved algorithm. Finally, taking the DEM map of a certain area as an example, the three-dimensional path planning simulation results of the improved algorithm and other five group intelligent algorithms are given to prove the superiority of the algorithm in actual engineering problems.

2. Mixed-Integer Programming Model for Three-Dimensional UAV Trajectory Planning

2.1 Problem Description

3D UAV path planning refers to the process of planning a safe, feasible, low-cost, and optimal continuous flight trajectory from a starting point to a target point within a 3D spatial environment, while comprehensively considering environmental constraints, the UAV's own flight constraints, performance limitations, and trajectory length. This paper simplifies threat regions in the real-world environment into cylinders and considers obstacle avoidance between the UAV and the cylinders.

2.2 Coordinate System Transformation

Taking into account the performance constraints of the UAV, this paper employs a spherical coordinate system to constrain the UAV's yaw angle ϕ and pitch angle ψ. In the spherical coordinate system (ρ, ψ, φ), ρ represents the distance of the flight segment, ψ represents the pitch angle, and ϕ represents the deflection angle. Given a trajectory consisting of n waypoints, once the waypoint coordinates Ω in the spherical coordinate system are obtained, they are converted to the Cartesian coordinate system to yield coordinates $P = (p_1, p_2, \cdots, p_n)$, where the i-th waypoint is $p_i = (x_i, y_i, z_i)$. The update method in the Cartesian coordinate system is as follows:

$$\begin{cases} x_i = x_{i-1} + \rho_i \sin\psi_i \cos\varphi_i \\ y_i = y_{i-1} + \rho_i \sin\psi_i \cos\varphi_i \\ z_i = z_{i-1} + \rho_i \cos\varphi_i \end{cases} \tag{1}$$

Since the resulting data consists of trajectory segments connecting multiple waypoints, B-spline curves are employed to smooth the trajectory and generate a smooth trajectory curve. The formula for the B-spline curve is as follows:

$$B(u) = \sum_{i=0}^{m-n-2} D_i N_{i,3}(v)\,, v \in [v_n, v_{m-n-1}] \tag{2}$$

In the formula, m is the number of nodes v; the values of v_i range over $\{z_0, z_1, \cdots z_{m-1}\}$ with $x_0 \leq x_1 \leq \cdots x_{m-1}$; D_i represents the control points, with a total of m-n-1 control points; and $N_{i,n}$ denotes the B-spline basis function of degree n, as shown in the following formula:

$$N_{i,1} = \begin{cases} 1, v_i \leq v \leq v_{i+1} \\ 0, others \end{cases} \tag{3}$$

$$N_{i,n}(v) = \frac{v - v_i}{v_{i+n} - v_i} N_{i,n-1}(v) + \frac{v_{i+n+1} - v_i}{v_{i+n+1} - v_{i+1}} N_{i+1,n-1(v)} \tag{4}$$

2.3 Objective Function

2.3.1 Total Trajectory Cost Function

For the problem of 3D trajectory planning for UAVs, it is necessary to consider constraints related to the UAV's own performance as well as those associated with mission execution. Therefore, based on actual flight conditions, this paper establishes a UAV trajectory planning model by comprehensively considering cost functions such as trajectory length, flight altitude, path smoothness, and threat region cost. The total trajectory cost function F is shown below:

$$F = \omega_1 \cdot f_1 + \omega_2 \cdot f_2 + \omega_3 \cdot f_3 + \omega_4 \cdot f_4 \tag{5}$$

$$\sum_{i}^{4} \omega_i = 1 \tag{6}$$

Where F is the total cost of the trajectory, f_1 represents the trajectory length cost, and f_2 represents the flight altitude cost; f_3 represents the cost associated with trajectory smoothness, and f_4 represents the cost associated with threat region cost; ω_i denotes the weighting coefficient for each cost function, and these weights can be dynamically adjusted based on the requirements of the flight mission and the flight environment.

2.3.2 Trajectory Length Cost Function

Trajectory path length is one of the key metrics for evaluating UAV path planning. A shorter trajectory reduces fuel consumption and operational costs, thereby enhancing economic efficiency. The formula is as follows:

$$f_1 = \sum_{i}^{n-1} L_i \tag{7}$$

$$L_i = \sqrt{(x_{i+1} - x_i)^2 + (y_{i+1} - y_i)^2 + (z_{i+1} - z_i)^2} \tag{8}$$

Where L_i is the length of the i-th trajectory segment, and (x_i, y_i, z_i) are the coordinates of the i-th trajectory point P_i.

2.3.3 Trajectory Altitude Cost Function

During flight, the altitude of the UAV is typically constrained between a minimum and a maximum value, denoted as h_{min} and h_{max}, respectively. The formula is as follows:

$$f_2 = \sum_{i}^{n} H_i \tag{9}$$

$$H_i = \begin{cases} \left| h_i - \frac{h_{\max} - h_{\min}}{2} \right|, h_{\min} \leqslant h_i \leqslant h_{\max} \\ \infty, others \end{cases} \tag{10}$$

In the formula, h_i is the flight altitude relative to the ground; $h_{\min}$ is the minimum required flight altitude for the UAV, and $h_{\max}$ is the maximum required flight altitude for the UAV.

2.3.4 Trajectory Smoothness Cost Function

Frequent path changes and altitude shifts can affect the safety and efficiency of drone flight. To ensure a smooth trajectory, yaw and pitch angles also need to be considered. The horizontal projection of the path segment from waypoint P_i to P_{i+1} can be represented by the vector $k_i = (X_{i+1} - X_i, Y_{i+1} - Y_i)$. Let ϕ_{max} denote the maximum deflection angle and ψ_{max} the maximum pitch angle. The calculations for the deflection and pitch angles, along with the cost function f_3 for path smoothness, are as follows:

$$f_3 = a_1 \sum_{i=1}^{n-1} \phi_i + a_2 \sum_{i=1}^{n-1} \varphi_i \tag{11}$$

$$\phi = \begin{cases} \arccos\left(\frac{k_i^T k_{i+1}}{|k_i||k_{i+1}|}\right), \phi < \phi_{\max} \\ \phi_{\max}, others \end{cases} \tag{12}$$

$$\varphi = \begin{cases} \arctan\left(\frac{|Z_i + 1 - Z_i|}{\sqrt{(X_{i+1} - X_i)^2 + \sqrt{(Y_{i+1} - Y_i)^2}}}\right), \varphi < \varphi_{\max} \\ \varphi_{\max}, others \end{cases} \tag{13}$$

In the formula, a_1 and a_2 are the penalty coefficients for the deflection angle and pitch angle, respectively; X_i, Y_i, and Z_i correspond to the x-, y-, and z-coordinates of the trajectory point in the Cartesian coordinate system, respectively.

2.3.5 Threat Region Cost Function

Trajectory planning also requires guiding the UAV to bypass obstacle zones within the 3D environment to ensure safe flight; the threat cost function is as follows:

$$f_4 = \sum_{i=1}^{n-1} \sum_{k=1}^{K} T_k(l_i) \tag{14}$$

$$T_k(l_i) = \begin{cases} 0, & d_k > S + D + R_k \\ S + D + R_k - d_k, & D + R_k < d_k \leq S + D + R_k \\ \infty, & d_k \leq D + R_k \end{cases} \tag{15}$$

In the formula, C_k is the coordinate of the threat center, R_k is the radius of the threat's central zone, and D and S represent the lateral dimensions of the collision zone and the danger zone, respectively; for a given trajectory l, the distance to the threat center C_k is d_k, as shown in Figure 1.

Figure 1: Navigation Threat Map

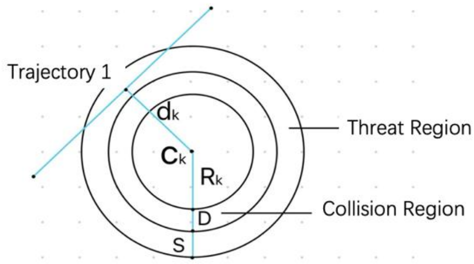

3. Multi-Strategy Chaos-Enhanced Grey Wolf Optimizer

3.1 Grey Wolf Optimizer

GWO performs global optimization by simulating the social structure and hunting behavior of grey wolves. It offers advantages such as a clear hierarchical structure, ease of implementation, and strong generalization capabilities. Currently applied in fields like scheduling and industry, it stands as a representative example of swarm intelligence algorithms. In the GWO algorithm, grey wolves are categorized into a hierarchy comprising α, β, δ, and ω wolves; each rank has clearly defined roles, and they collaborate to carry out hunting tasks. Among them, the α wolf is the leader of the population and is responsible for leading hunting tasks; in the algorithm, this is represented by the solution yielding the best result and the optimal fitness value. The β wolf assists the α wolf in decision-making, playing a supporting role within the pack; in the algorithm, this is reflected in the solution being suboptimal. The δ wolf follows the decisions of the α and β wolves and carries out specific actions; The ω wolf represents the remaining grey wolves in the population; they strictly obey the commands of the top three and follow them during hunting operations, possessing the lowest fitness value in the algorithm.

In the optimization algorithm, the prey's position corresponds to the global optimum of the optimization problem, while the α, β and δ wolves represent the best, second-best, and third-best solutions found so far, serving as benchmarks for locating the prey. The Grey Wolf Optimizer consists of two phases: encircling and hunting.

Encirclement phase. The gradual approach to and encirclement of the prey are achieved through the following formula.

$$D = |\mathrm{C} \cdot \mathrm{X_p(t)} - \mathrm{X(t)}| \tag{16}$$

$$\mathrm{X}(t+1) = X_P(t+1) - A \cdot D \tag{17}$$

$$A = 2a \cdot r_1 - a \tag{18}$$

$$C = 2 \cdot r_2 \tag{19}$$

In the equation, t is the current iteration number; $X_P(t)$ is the position vector of the prey at the t-th generation, corresponding to a candidate optimal solution for the optimization problem; $\mathrm{X}(t)$ is the position vector of a grey wolf individual at generation t; D is the distance between the grey wolf individual and the prey. A and C are coefficients; coefficient A controls the movement direction of the grey wolves, while coefficient C controls the influence weight of the target wolf. a is the convergence factor that controls the algorithm's global search and local exploitation, decreasing linearly from 2 to 0 as the number of iterations increases; r_1 and r_2 are random numbers between 0 and 1.

The pursuit phase. Other grey wolves in the population estimate the prey's location based on the positions of the α, β and δ wolves; they move toward these three leaders, calculate their respective distances from them, and update their own positions. The formulas are as follows.

$$\begin{cases} D_\alpha = \mid \mathrm{C_1} \cdot \mathrm{X_\alpha} - \mathrm{X} \mid \\ D_\beta = \mid \mathrm{C_2} \cdot \mathrm{X_\beta} - \mathrm{X} \mid \\ D_\delta = \mid \mathrm{C_3} \cdot \mathrm{X_\delta} - \mathrm{X} \mid \end{cases} \tag{20}$$

$$\begin{cases} X_1 = X_\alpha - A_1 \cdot D_\alpha \\ X_2 = X_\beta - A_2 \cdot D_\beta \\ X_3 = X_\delta - A_3 \cdot D_\delta \end{cases} \tag{21}$$

$$X(t+1) = \frac{X_1 + X_2 + X_3}{3} \tag{22}$$

In the equation, X_α, X_β and X_δ are the position vectors of the α, β and δ wolves, respectively; D_α, D_β and D_δ are the distances between the individual gray wolf and the α, β and δ wolves, respectively; X_1, X_2 and X_3 are the candidate positions of the individual gray wolf after moving towards the α, β and δ wolves; and $X(t+1)$ is the final position of the individual gray wolf at generation $t+1$.

3.2 Improvement Strategies

In view of the shortcomings of GWO such as uneven distribution of search areas, low algorithm convergence accuracy, and easy falling into local optimality, GWO is integrated with chaotic map, nonlinear parameters, golden sine strategy, etc. The specific process is as follows:

3.2.1 Tent–Logistic Hybrid Chaotic Map

To address the limitations of the Grey Wolf Optimizer (GWO)—specifically, the inability of its initial-stage random search to fully explore the solution space and the uneven distribution of the search range—a hybrid Tent-Logistic map is introduced. This modification enhances the randomness of the exploration step size in each iteration, thereby increasing the probability of finding the global optimum and accelerating the algorithm's convergence speed.

The Logistic chaotic map is a representative model in chaotic dynamics. Logistic chaotic sequences exhibit strong global ergodicity; incorporating the Logistic chaotic map into the Grey Wolf Optimizer enhances spatial search capabilities and improves search accuracy. Its mathematical expression is:

$$X_{k+1} = \mu \cdot X_k \cdot (1 - X_k) \tag{23}$$

In the equation, X_k and X_{k+1} are the position vectors of the grey wolf at times k and $k+1$, respectively, and μ is a control parameter ranging from 0 to 4; when $\mu = 4$, the Logistic map is in a completely chaotic state.

Compared to the Logistic map, the Tent map features a uniform probability density and power spectral density, ideal correlation properties, and rapid convergence. Combining the Tent chaotic map with the Grey Wolf Optimizer algorithm can accelerate the algorithm's convergence speed and improve its search efficiency; the expression is as follows:

$$X_{k+1} = \begin{cases} 2X_k, & 0 \le X_k \le 0.5 \\ 2(1 - X_k), & 0.5 < X_k \le 1 \end{cases} \tag{24}$$

Where X_k and X_{k+1} are the position vectors of the grey wolf at times k and $k+1$, respectively.

3.2.2 Nonlinear Parameter Update

The original GWO algorithm employs a linearly decreasing control parameter a, but this approach fails to meet the algorithm's requirements for solving complex problems. Therefore, this paper proposes a nonlinear control parameter strategy capable of meeting the requirements for global exploration and local exploitation, as formulated below:

$$a_m = a\left[1-\left(\frac{e^{\frac{t}{T_m}}-1}{e-1}\right)^k\right] \tag{25}$$

In the formula, a is the initial value of the convergence factor, and k is an adjustment parameter, typically ranging from 0 to 6.

3.2.3 Golden Sine Strategy

To address the drawback of the GWO population easily falling into local optima during the exploitation phase, the Golden Sine strategy is employed to perturb the positions of the grey wolves, thereby facilitating the algorithm's search for better positions. The position update formula for the Grey Wolf Optimizer based on the golden sine strategy is as follows:

$$X_i' = X_i|\sin(r_1)| + r_2\sin(r_2)|c_1B - c_2X_i| \tag{26}$$

In the formula, r_1 and r_2 are random numbers taking values in the ranges [0,2π] and [0,π] respectively, representing the movement distance and direction of the next-generation individual; c_1 and c_2 are golden section parameters used to reduce the search space and guide individuals to converge toward the optimal value; and B is the position of the optimal individual. The golden section parameters c_1 and c_2 are set using Equations (27) and (28).

$$c_1 = a \times (1-\mu) + b \times \mu \tag{27}$$

$$c_2 = a \times \mu + b \times (1-\mu) \tag{28}$$

In the formula, a is set to $-\pi$, b to π, and μ is the golden ratio, approximately equal to 0.618.

4. Algorithm Performance Evaluation and Analysis

To evaluate the performance of the improved algorithm, the MSCEGWO proposed in this paper was compared against the standard GWO, Dung Beetle Optimizer (DBO), Hiking Optimization Algorithm (HOA), Particle Swarm Optimization (PSO), and Sparrow Search Algorithm (SSA) using benchmark functions; for all algorithms, the population size was set to 50 and the number of iterations to 500. The simulation environment utilized the Windows 11 64-bit operating system with 16 GB of RAM, and MATLAB R2021b served as the simulation software.

4.1 Benchmark Functions and Parameter Settings

Twelve benchmark functions were selected for the experiment; their dimensions, domains, and optimal values are listed in Table 1. In the table, F1 through F5 are unimodal test functions primarily used to evaluate the solution accuracy of the algorithms, while F6 through F12 are multimodal functions primarily used to assess the algorithms' ability to escape local optima. The improved MSCEGWO algorithm is compared with other intelligent optimization algorithms using test functions, with their optimal values, standard deviations, and mean values calculated. The first metric serves to verify the algorithm's exploration capability, while the latter two assess its convergence accuracy and stability. To avoid the randomness associated with a single trial and to enhance the persuasiveness of the experiments, the different algorithms were independently run 30 times on these test functions, and the final results were obtained by averaging the outcomes.

4.2 Comparison of Benchmark Function Results

The comparative experimental results of different algorithms are shown in Table 2. Overall, the MSCEGWO algorithm is superior to or equal to other algorithms in the three aspects of optimal value, mean value and standard deviation of 11 test functions.

Specifically, in the single-peak function, the optimal value and mean value of MSCEGWO's solution from F1 to F3 are 0, indicating that the nonlinear parameter update strategy of the algorithm can more accurately seek a better solution in the later stage, which greatly improves the solution accuracy of the algorithm. Although the sparrow search algorithm (SSA) can also converge to the theoretical optimal value of 0 in the test functions F1 and F2, its average and standard deviation are not 0, indicating that the stability of SSA is not as good as that of MSCEGWO.

In multimodal functions, compared with most algorithms, the optimal value of MSCEGWO can reach the best. For complex multi-peak test functions such as test functions F9 to F11, the theoretical optimum is also achieved, which reflects that the application of golden sinusoidal strategy in algorithms greatly improves the solution stability of the algorithm in complex situations and the ability to avoid local optima.

Table 1: Test Functions

Function Category	No.	Function	Dimension	Search Range	Optimal Value
	F1	Shifted Schwefel's Problem 1.2	30	[-10,10]	0
	F2	Shifted Rotated High Conditioned Elliptic Function	30	[-100,100]	0
Unimodal Benchmark Functions	F3	Shifted Schwefel's Problem 1.2 with Noise in Fitness	30	[-100,100]	0
	F4	Shifted Rotated Griewank's Function without Bounds	30	[-1.28,1.28]	0
	F5	Rotated Hybrid Composition Function with the Global Optimum on the Bounds	4	[0,10]	-10.4029
	F6	Shifed and Rotated Bent Cigar Function	20	[-100,100]	0
	F7	Hybrid Function 1(N=3)	20	[-100,100]	0
	F8	Hybrid Function 3(N=5)	20	[-100,100]	0
Multimodal Benchmark Functions	F9	Composition Function 2(N=4)	20	[-100,100]	0
	F10	Composition Function 3(N=5)	20	[-100,100]	0
	F11	Storn's Chebyshev Polynomial Fitting Problem	9	[-8192,8192]	1
	F12	Inverse Hilbert Matrix Problem	16	[-6384,6384]	1

Table 2: Comparison of MSCEGWO and classical optimization algorithms for finding the best

Benchmark Function	Statistic	MSCEGWO	GOA	DBO	GWO	PSO	SSA
	Best Value	0.00E+00	1.48E-15	1.11E-85	5.11E-42	4.60E-08	0.00E+00
F1	Standard Deviation (Std.)	0.00E+00	1.40E-14	1.29E-47	6.75E-40	2.08E-07	5.86E-67
	Mean	0.00E+00	1.44E-14	2.36E-48	4.31E-40	2.66E-07	1.07E-67
	Best Value	0.00E+00	5.66E-27	1.96E-165	2.07E-38	2.86E-05	0.00E+00
F2	Standard Deviation (Std.)	0.00E+00	2.18E-24	2.46E-90	1.24E-31	3.76E-04	1.74E-91
	Mean	0.00E+00	1.19E-24	5.51E-91	3.83E-32	3.53E-04	3.18E-92
	Best Value	0.00E+00	6.86E-16	1.31E-81	9.27E-25	4.71E-05	7.73E-194
F3	Standard Deviation (Std.)	0.00E+00	1.65E-14	6.40E-54	1.82E-22	3.56E-04	3.76E-61
	Mean	0.00E+00	1.87E-14	1.67E-54	1.65E-22	4.56E-04	6.86E-62
	Best Value	1.43E-06	8.00E-06	8.70E-05	1.88E-05	3.98E-04	1.38E-05
F4	Standard Deviation (Std.)	2.48E-05	1.86E-04	9.41E-04	2.27E-04	1.13E-03	3.17E-04
	Mean	3.00E-05	2.82E-04	1.40E-03	3.42E-04	2.10E-03	4.32E-04
	Best Value	-1.04E+01	-1.04E+01	-1.04E+01	-1.04E+01	-1.04E+01	-1.04E+01
F5	Standard Deviation (Std.)	7.63E-02	1.16E+00	2.78E+00	6.81E-04	3.52E+00	2.01E+00

Benchmark Function	Statistic	MSCEGWO	GOA	DBO	GWO	PSO	SSA
	Mean	-1.03E+01	-9.09E+00	-6.88E+00	-1.04E+01	-7.44E+00	-9.52E+00
	Best Value	0.00E+00	3.98E-24	7.63E-160	2.37E-41	8.32E+00	0.00E+00
F6	Standard Deviation (Std.)	0.00E+00	1.19E-20	4.53E-114	1.06E-37	1.87E+03	3.27E-109
	Mean	0.00E+00	6.97E-21	8.27E-115	8.15E-38	4.19E+02	5.97E-110
	Best Value	0.00E+00	5.88E-20	5.42E-150	2.16E-21	2.41E+01	0.00E+00
F7	Standard Deviation (Std.)	0.00E+00	7.41E-18	4.71E+01	6.07E+00	1.31E+04	5.50E-19
	Mean	0.00E+00	5.53E-18	1.31E+01	2.92E+00	2.80E+03	1.00E-19
	Best Value	-2.22E-16	3.89E-06	1.49E-30	1.38E-02	2.06E+00	-2.22E-16
F8	Standard Deviation (Std.)	1.13E-16	1.19E-04	4.56E+01	9.33E-01	2.49E+02	1.36E-07
	Mean	-1.18E-16	1.12E-04	1.12E+01	5.12E-01	2.60E+02	2.48E-08
	Best Value	0.00E+00	8.88E-15	3.12E-168	1.78E-14	7.49E-03	0.00E+00
F9	Standard Deviation (Std.)	0.00E+00	1.31E-13	3.85E-78	8.39E-15	1.16E-02	3.87E-88
	Mean	0.00E+00	1.60E-13	7.03E-79	2.43E-14	2.22E-02	9.33E-89
	Best Value	0.00E+00	4.07E-04	9.21E-06	7.83E-03	4.93E+01	0.00E+00
F10	Standard Deviation (Std.)	0.00E+00	2.96E+01	4.21E+01	1.88E+01	1.29E+01	1.80E-15
	Mean	0.00E+00	5.40E+00	4.84E+01	7.02E+01	5.97E+01	4.74E-16
	Best Value	1.00E+00	1.00E+00	1.00E+00	1.00E+00	3.65E+03	1.00E+00
F11	Standard Deviation (Std.)	0.00E+00	1.12E-08	3.93E+05	4.38E+04	2.64E+05	0.00E+00
	Mean	1.00E+00	1.00E+00	2.01E+05	1.73E+04	3.06E+05	1.00E+00
	Best Value	4.28E+00	4.61E+00	4.22E+00	2.55E+01	1.45E+02	4.21E+00
F12	Standard Deviation (Std.)	2.97E-01	1.06E+00	7.88E+03	2.69E+02	1.07E+02	1.38E-01
	Mean	4.81E+00	5.14E+00	4.85E+02	4.28E+02	3.64E+02	4.28E+00

4.3 Analysis of Convergence Curves and Boxplots

The convergence curve of 12 test functions solved by different algorithms is shown in Figure 2. The convergence curve of MSCEGWO is smoother and the convergence curve has a steeper slope. In most test functions, the first 300 iterations have reached the optimal value, which indicates that MSCEGWO has the fastest convergence speed.

In addition, the box plot of each algorithm to box plots of different algorithms on the benchmark functions is shown in Figure 3. It can be seen that the average and standard deviation of MSCEGWO is relatively small, reflecting the good optimization performance and stability of the algorithm.

Figure 2: Comparison chart of convergence of functions

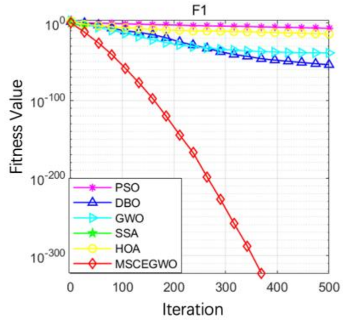

Convergence Curve of F1

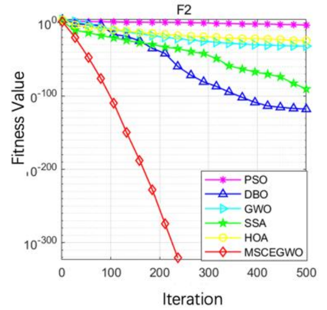

Convergence Curve of F2

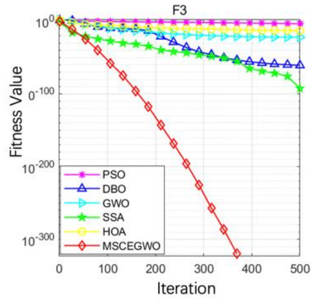

Convergence Curve of F3

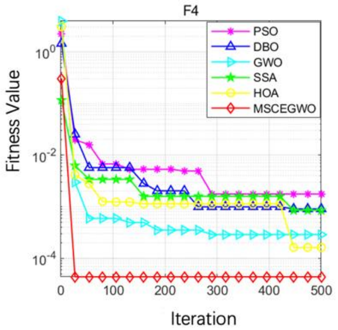

Convergence Curve of F4

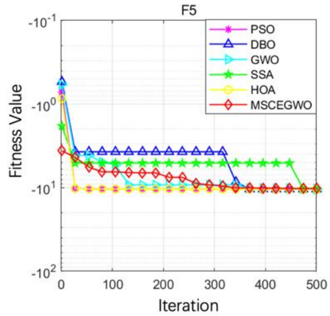

Convergence Curve of F5

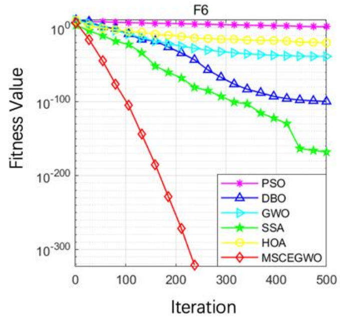

Convergence Curve of F6

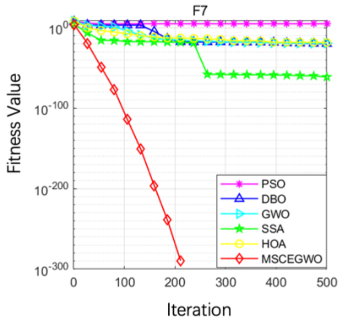

Convergence Curve of F7

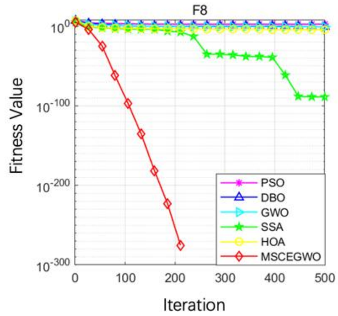

Convergence Curve of F8

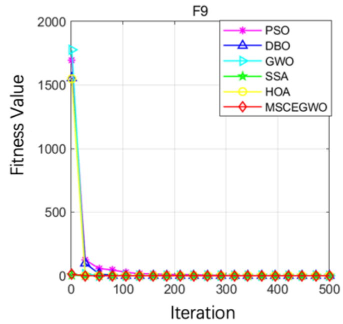

Convergence Curve of F9

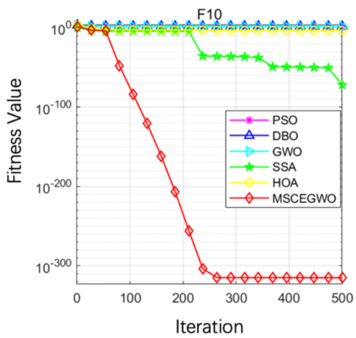

Convergence Curve of F10

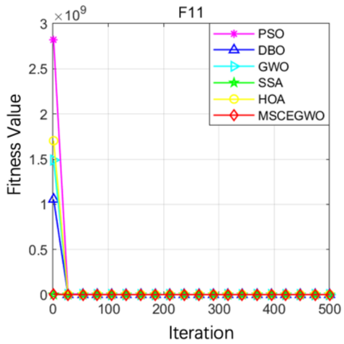

Convergence Curve of F11

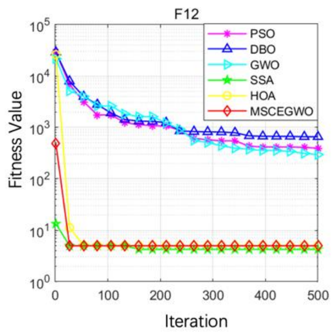

Convergence Curve of F12

Figure 3: Algorithm box plot

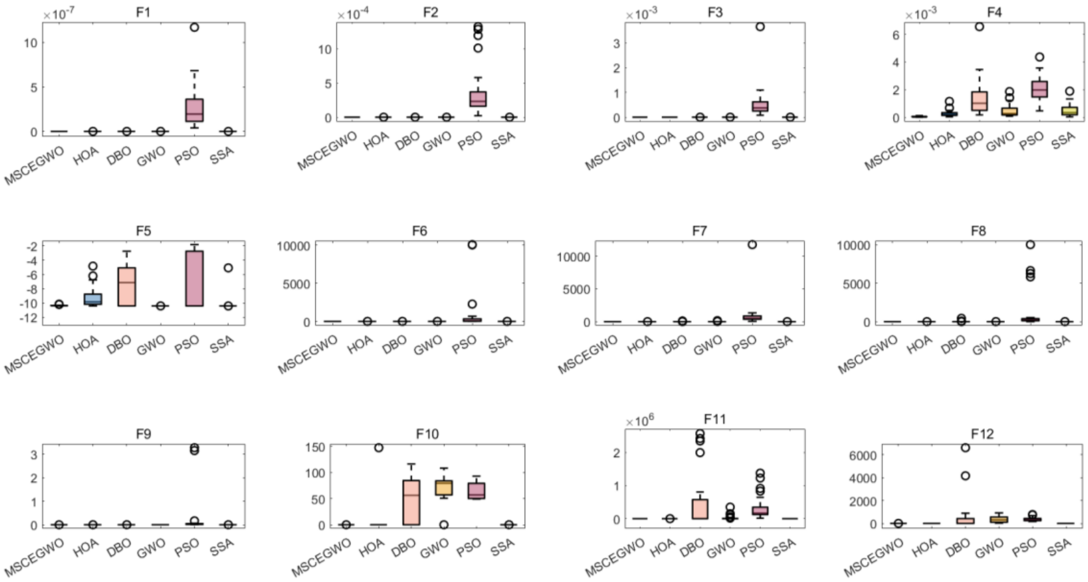

4.4 Wilcoxon Rank-Sum Test

This paper uses the Wilcoxon rank-sum test and the p-value to verify whether the improved MSCEGWO is significantly different from the other five algorithms. Significant differences show that the improvement strategy of the algorithm is effective and can significantly improve the solution accuracy and speed of the algorithm.

If $p < 0.05$, there is a significant difference between the two algorithms. N/A means that the performance of the two algorithms is equivalent and optimal. "+/=/–" indicates that MSCEGWO is "better than/comparable to/worse than" to other algorithms in terms of performance. It can be seen from Table 3 that most of the p values of MSGOA in F1-F12 are less than 0.05 and are "+", indicating that MSCEGWO has better performance than other five algorithms. Among them, MSCEGWO and DBO have the same performance in global optimization in F5, and both achieve the theoretical optimum; MSCEGWO has significant differences from all test functions of GWO, which shows that the improvement strategy is very important for algorithm improvement.

Table 3: p value of Wilcoxon rank-sum test

Benchmark Function	GOA	DBO	GWO	PSO	SSA
F1	1.21E-12	1.21E-12	1.21E-12	1.21E-12	1.66E-11
F2	1.21E-12	1.21E-12	1.21E-12	1.21E-12	6.25E-10
F3	1.21E-12	1.21E-12	1.21E-12	1.21E-12	1.21E-12
F4	2.92E-09	3.02E-11	1.78E-10	3.02E-11	1.07E-09
F5	1.56E-08	N/A	4.98E-11	N/A	6.36E-06
F6	1.21E-12	1.21E-12	1.21E-12	1.21E-12	6.25E-10
F7	1.21E-12	1.21E-12	1.21E-12	1.21E-12	1.93E-10
F8	2.21E-11	2.21E-11	2.21E-11	2.21E-11	6.55E-04
F9	3.01E-11	3.02E-11	1.45E-11	3.02E-11	1.06E-07
F10	3.02E-11	3.02E-11	3.02E-11	3.02E-11	8.48E-09
F11	4.57E-12	6.24E-10	1.21E-12	1.21E-12	N/A
F12	N/A	1.24E-05	1.44E-11	1.44E-11	1.86E-10
+/=/-	11/1/0	11/1/0	12/0/0	11/1/0	11/1/0

5. Simulation Experiments for Three-Dimensional UAV Trajectory Planning

Taking a DEM with a spatial resolution of 30 m for a specific area as an example, the obstacle parameters are listed in Table 4, and a 3D visualization of the environment is shown in Figure 4; the environment contains six static obstacles. The coordinates of the task's start and end points are (200, 100, 150) and (800, 800, 150), respectively. In addition, the weights for the four cost objective functions are set to 100, 80, 120, and 50, respectively, while the penalty coefficients a and b for the horizontal steering angle and vertical pitch angle are both set to 50.

The MSCEGWO proposed in this paper and five other swarm intelligence algorithms were applied to solve the UAV 3D path planning model; The experimental results are shown in Figure 6 and Table 5. The convergence curves of each algorithm to solve the UAV track is shown in Figure 7. It can be seen from this: (1) MSCEGWO can accelerate the convergence speed of the algorithm by using tent-logistic hybrid mapping to initialize the population, and the average number of iterations is less than that of the original gray wolf optimization algorithm. (2) MSCEGWO uses nonlinear functions to update algorithm parameters in the exploration stage to expand the global optimization ability of the algorithm. The planned path improved by MSCEGWO is smoother and can find a better path in the middle of the obstacle. (3) MSCEGWO finally uses the golden sinusoidal strategy to prevent the algorithm from falling into local optima, which is improves the solution accuracy. The total path cost of the path generated by MSCEGWO is the lowest, indicating that the path it generates is the best. The average total cost value is reduced by 12.49% compared with the original algorithm.

Table 4: Environmental Constraint Parameters

No.	Coordinates	Radius	Type
1	[400,500,0]	50	Static Obstacle
2	[600,200,0]	40	Static Obstacle
3	[500,350,0]	50	Static Obstacle
4	[350,200,0]	40	Static Obstacle
5	[700,550,0]	40	Static Obstacle
6	[650,750,0]	50	Static Obstacle

Table 5: Performance comparison of different algorithms for UAV trajectory planning

Algorithm	Average Number of Iterations	Average Total Cost	Percentage of Total Cost of MSCEGWO (%)	Trajectory Length Cost	Threat Region Cost	Altitude Cost	Smoothness Cost
MSCEGWO	46	9187	100	3674	1837	1610	2066
GOA	39	10529	87.3	4211	2105	1837	2376
DBO	22	9568	96.0	3827	1913	1382	2446
GWO	53	10498	87.5	4199	2099	1633	2567
PSO	66	10195	90.1	4078	2039	1786	2292
SSA	67	11408	80.5	4563	2281	1683	2881

Figure 4: 3D visualization of the optimal flight path

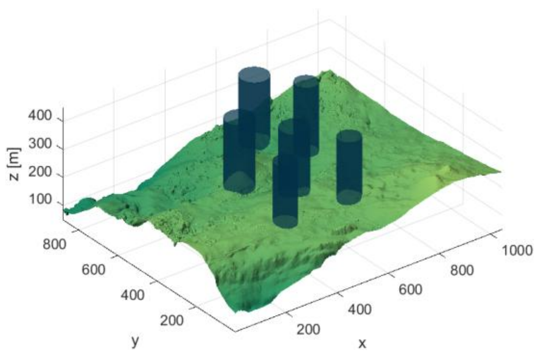

Figure 5: Top View of UAV Path Planning

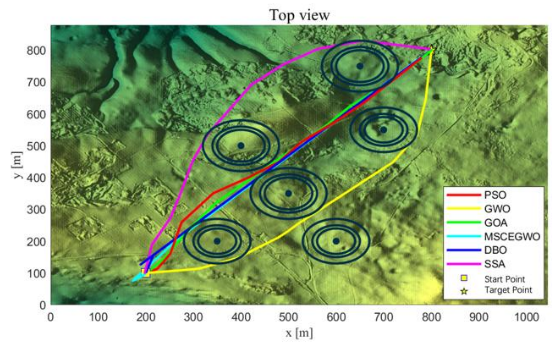

Figure 6: Side View of UAV Path Planning

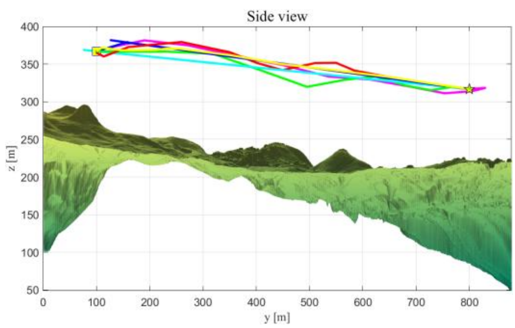

Figure 7: Front View of UAV Path Planning

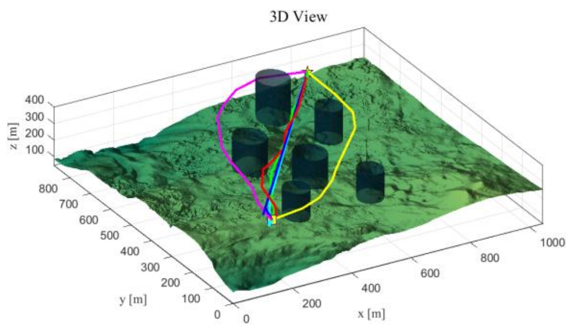

Figure 8: Iterative curve of different algorithms for solving UAV tracks

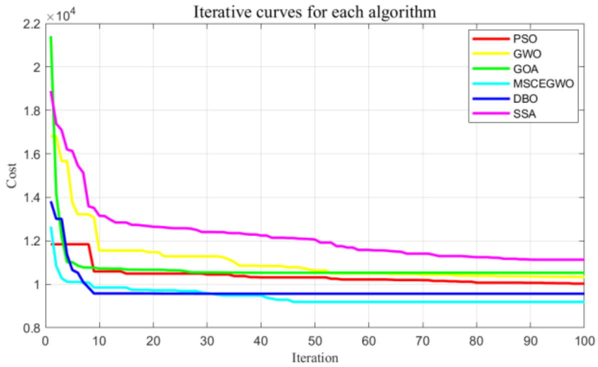

6. Conclusions

In response to the problems that the classic gray wolf optimization algorithm is easy to fall into local optima, low solution accuracy and slow convergence speed in the process of drone three-dimensional path planning, this paper proposes a multi-strategy chaos-enhanced gray wolf optimization algorithm. Compare this improved algorithm with other five mainstream swarm intelligence algorithms in the standard test function, and give the three-dimensional path planning simulation results of this improved algorithm and other five algorithms. Verify the effectiveness of MSCEGWO's improvement strategy from multiple angles. Research shows that:

(1) The MSCEGWO in this paper uses tent-logistic hybrid mapping to generate diverse initial populations, the nonlinear function update algorithm parameters to expand the global exploration ability of the algorithm, and the golden sinusoidal strategy to prevent the algorithm from falling into local optimization. Compared with other group intelligence algorithms, MSCEGWO has better convergence accuracy and speed.

(2) MSCEGWO can achieve better results in real engineering problems. In the three-dimensional path planning problem of unmanned aerial vehicles, the planned path of MSCEGWO is better than the planned path of other algorithms, and the average path cost is reduced by 12.49% compared with the original algorithm. The path generated by MSCEGWO is conducive to ensuring the safety of unmanned aerial vehicle flight, improving the efficiency of unmanned aerial vehicle flight, and increasing economic benefits.

The shortcomings of this article include: (1) It does not involve the path planning of multiple drones; (2) The real-time path planning of the drone and the impact of dynamic obstacles are not taken into account. (3) The relationship between the UAV's own structure and the track is not considered. These are our future research directions.

References

[1] Jiang, Q., & Wu, K. (2026). Three-dimensional UAV trajectory planning based on an improved bat algorithm. *Dianguang Yu Kongzhi* [Journal of Electro-Optics and Control], Advance online publication. https://link.cnki.net/urlid/41.1227.tn.20260319.0917.002

[2] Chen, Y., & Wu, D. (2025). Three-dimensional UAV path planning based on an improved hybrid Grey Wolf Optimizer. *Journal of Ningbo University of Technology, 37*(3), 11–20.

[3] Wang, W., Hu, J., Chen, L., Zhou, T., et al. (2026). Three-dimensional UAV trajectory planning based on an improved marine predator algorithm. *Binggong Xuebao (Acta Armamentarii), 47*(1), 221–236.

[4] Mirjalili, S., Mirjalili, S. M., & Lewis, A. (2014). Grey wolf optimizer. *Advances in Engineering Software, 69*, 46–61.

[5] Dorigo, M., Birattari, M., & Stützle, T. (2006). Ant colony optimization. *IEEE Computational Intelligence Magazine, 1*(4), 28–39.

[6] Kennedy, J., & Eberhart, R. C. (1995). Particle swarm optimization. In *Proceedings of the IEEE International Conference on Neural Networks* (Vol. 4, pp. 1942–1948). IEEE.

[7] Qin, D., Yan, X., Shao, G., et al. (2025). Three-dimensional trajectory planning for quadrotor UAVs based on an event-triggered Grey Wolf Optimizer. *CAAI Transactions on Intelligent Systems, 20*(3), 699–706.

[8] Chen, M., Zhou, Z., Zhang, Y., et al. (2025). Three-dimensional UAV trajectory planning based on an improved RRT* algorithm. *Journal of Ordnance Equipment Engineering, 46*(4), 192–199, 234.

[9] Shen, C., Zhang, H., & Cai, P. (2025). Three-dimensional trajectory planning for plant protection UAVs based on an improved ant colony algorithm. *Journal of Chinese Agricultural Mechanization, 46*(2), 113–119. https://doi.org/10.13733/j.jcam.issn.2095-5553.2025.02.017

[10] Liu, W., & Li, T. (2024). UAV trajectory planning based on an improved dung beetle optimizer. *Electronic Measurement Technology, 47*(15), 64–72. https://doi.org/10.19651/j.cnki.emt.2416358

[11] Wang, Y., Song, J., Zhao, H., et al. (2026). A review of research and applications of the Grey Wolf Optimizer. *Ruanjian Daokan* [Software Guide], Advance online publication. https://link.cnki.net/urlid/42.1671.TP.20260206.1346.004

[12] Wang, S., Hua, G., Hao, G., et al. (2017). Application of a Grey Wolf Optimizer-based long short-term memory network for time series prediction. *China Sciencepaper, 12*(20), 2309–2314.

[13] Bao, X., Gao, H., Zhou, R., et al. (2025). Design of a low-frequency oscillation suppression strategy for power systems based on the Grey Wolf Optimizer. *Electrical Industry, 2025*(4), 35–39.

[14] Wang, Q., Li, C., & Liu, T. (2025). Three-dimensional UAV trajectory planning based on an improved Grey Wolf Optimizer. *Changjiang Information & Communications, 38*(10), 57–60. https://doi.org/10.20153/j.issn.2096-9759.2025.10.016

[15] Wang, H., Deng, J., Zhang, Y., et al. (2024). Three-dimensional UAV path planning based on an improved hybrid Grey Wolf Optimizer. *Radio Engineering, 54*(4), 918–927.

Funding

This research received no external funding.

Conflicts of Interest

The authors declare no conflict of interest.

Acknowledgment

This paper is an output of the science project.